SEPARATION OF LOW-FREQUENCY WAVES BY AN ANALYTICAL METHOD

Yuxiang Ma[1], Guohai Dong[2], Xiaozhou Ma[3]

A new method for separating low-frequency waves in time domain is proposed by constructing the analytical signals of the measured waves. Using three simultaneous wave records, the time series of incident bound, free and reflected low-frequency waves can be obtained by the present method. This method is only suitable for separating monochromatic low-frequency waves. The applicability of the method is examined by numerical tests. The results show that the present method can give accurate results over sloping beaches when water depth (*kh*) is larger than 0.2. Then, the present method is used to study an experiment of low-frequency waves over a mild slope beach.

Keywords: low-frequency wave; separation technique; analytic signal

INTRODUCTION

Waves in the infragravity frequency band are an important wave motion in the coastal zone. Many researches have shown that low-frequency waves or infragravity waves can lead to resonant responses of harbors (Bowens, 1977) and moored ships (Nagai et al., 1994), have important role in the coastal morphology process (Yu and Mei, 2000), and have significant influence on the design of coastal structures (Kamphuis, 2000).

Among the generation mechanisms of these low-frequency waves, release of *bound* subharmonic waves (Longuet-Higgins and Stewart, 1962) and moving breaking points (Symonds et al., 1982) are widely recognized. Separating low-frequency waves into specific components (i.e. incident free long waves, reflected free long waves and incident bound long waves) is vital to analyze the low-frequency waves and realize the generation mechanism of these low-frequency waves (Baldock et al., 2000). Several methods (e.g., Kostence, 1984; Bakkenes, 2002) are available for separating low-frequency waves. However, based on Fourier transform, the amplitude and phase information in time can not be directly obtained by these methods.

In this paper, a new method is proposed for separating low-frequency waves over sloping bathymetries in the real-time domain by constructing the analytical signals of the low-frequency waves measured simultaneously at three spaced locations. Hence, the amplitude and phase information of low-frequency waves in time can be obtained.

SEPARATION PRINCIPLE

The schematic diagram for the separation method is shown in Figure 1. The mean position of the wave maker is defined as x = 0 m. Three wave gauges, which are located at x_1, x_2 and x_3, are used to record the surface elevations simultaneously. The space between x_1 and x_2 is Δx, and the space between x_2 and x_3 is $\delta\Delta x$, where δ is a nondimensional value larger than 0.

[1] State Key Laboratory of Coastal and Offshore Engineering, Dalian University of Technology, Dalian, 116023, P.R. China
[2] State Key Laboratory of Coastal and Offshore Engineering, Dalian University of Technology, Dalian, 116023, P.R. China
[3] State Key Laboratory of Coastal and Offshore Engineering, Dalian University of Technology, Dalian, 116023, P.R. China

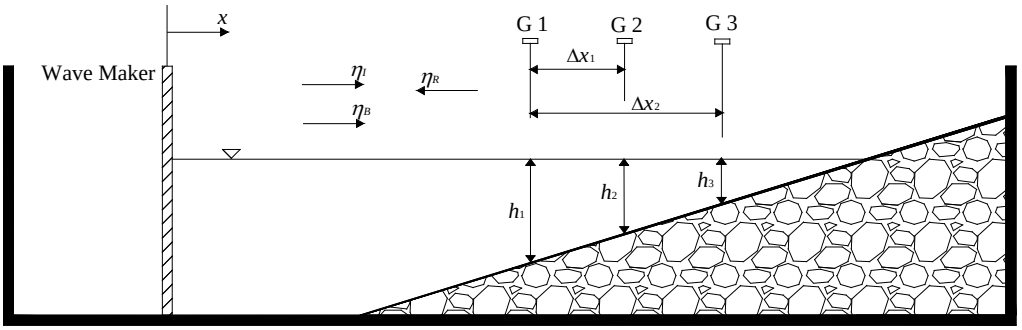

Figure 1. Schematic diagram for separating low-frequency waves over a sloping bathymetry.

In a study of low-frequency waves generated by bichromatic wave groups, which are composed by waves with frequency ω_1 and ω_2, the low-frequency wave series with frequency $\Delta\omega$ ($\Delta\omega = |\omega_1 - \omega_2|$) can be obtained by a band-pass filter. Generally, the measured low-frequency waves are composed by the incident free long waves, η_I, the reflected free long waves, η_R, and the incident bound long waves, η_B. The amplitude changes between the measured locations are determined using the linear shoaling theory. Then, the low-frequency waves at the three wave gauges can be expressed as:

$$\begin{aligned}\eta(x_1,t) = {} & a_I \cos(\Delta\omega t - \kappa_1 x_1 + \phi_I) \\ & + a_R \cos(\Delta\omega t + \kappa_1 x_1 + \phi_R) \\ & + a_B \cos(\Delta\omega t - \Delta k_1 x_1 + \phi_B)\end{aligned} \tag{1}$$

$$\begin{aligned}\eta(x_2,t) = {} & ks_1 a_I \cos(\Delta\omega t - \kappa_2 x_2 + \phi_I) \\ & + ks_1 a_R \cos(\Delta\omega t + \kappa_2 x_2 + \phi_R) \\ & + ks_1 a_B \cos(\Delta\omega t - \Delta k_2 x_2 + \phi_B)\end{aligned} \tag{2}$$

$$\begin{aligned}\eta(x_3,t) = {} & ks_2 a_I \cos(\Delta\omega t - \kappa_3 x_3 + \phi_I) \\ & + ks_2 a_R \cos(\Delta\omega t + \kappa_3 x_3 + \phi_R) \\ & + ks_2 a_B \cos(\Delta\omega t - \Delta k_3 x_3 + \phi_B)\end{aligned} \tag{3}$$

where κ is the local wave number of free long waves and determined by the linear dispersion relation:

$$\Delta\omega^2 = g\kappa \tanh \kappa h \tag{4}$$

Δk is the wave number of incident bound waves and equal to the difference of the local wave numbers of the two primary waves; a_I , a_R and a_B are the amplitudes of the incident, reflected and bound long waves, respectively, and ϕ_I , ϕ_R and ϕ_B are the corresponding phases. ks_1 is the amplitude ratio between waves at x_1 and x_2, and ks_2 is the amplitude ratio between waves at x_1 and x_3, and both of them are determined by shoaling coefficient:

$$ks_1 = \frac{K_{s2}}{K_{s1}}, \qquad ks_2 = \frac{K_{s3}}{K_{s1}} \tag{5}$$

It is difficult to separate long waves via Eqs. (1), (2) and (3) directly. However, through constructing the analytic signal, the phase changes of waves between the measured locations can be

extracted, then, the composed long waves can be separated easily. The analytic signals of the measured long waves can be constructed by the Hilbert transform (Cohen, 1995) or the Morlet wavelet transform (Mallat, 1999) and can be express as:

$$\zeta\left(x_1,t\right)=a_I e^{i\psi_I}+a_B e^{i\psi_B}+a_R e^{i\psi_I} \tag{6}$$

$$\begin{aligned}\zeta\left(x_2,t\right)=&ks_1 a_I e^{i\psi_I}e^{-i\kappa_{c1}\Delta x}\\&+ks_1 a_B e^{i\psi_B}e^{-i\Delta k_{c1}\Delta x}\\&+ks_1 a_R e^{i\psi_I}e^{i\kappa_{c1}\Delta x}\end{aligned} \tag{7}$$

$$\begin{aligned}\zeta\left(x_3,t\right)=&ks_2 a_I e^{i\psi_I}e^{-i\kappa_{c2}(1+\delta)\Delta x}\\&+ks_2 a_B e^{i\psi_B}e^{-i\Delta k_{c2}(1+\delta)\Delta x}\\&+ks_2 a_R e^{i\psi_I}e^{i\kappa_{c2}(1+\delta)\Delta x}\end{aligned} \tag{8}$$

$$\begin{aligned}\psi_I&=\Delta\omega t-\kappa_1 x_1+\phi_I\\\psi_B&=\Delta\omega t-\Delta k_1 x_1+\phi_B\\\psi_R&=\Delta\omega t+\kappa_1 x_1+\phi_R\end{aligned} \tag{9}$$

where i is the imaginary unit, κ_{c1}, $\Delta k_{c1}\Delta x$, κ_{c2} and $\Delta k_{c2}\Delta x$ are the wave number changes between the measured locations and can be determined by numerical integrals. By further deriving the Eqs. (6), (7) and (8), the analytical forms of the incident bound long waves, reflected and incident free long waves at x_1 can be obtained as follows:

$$\begin{aligned}a_B e^{i(\Delta\omega t-\Delta k_1 x_1+\phi_B)}=&\frac{-C_2\left[\zeta\left(x_1,t\right)e^{-i\kappa_{c1}\Delta x}-\zeta\left(x_2,t\right)/ks_1\right]}{C_1C_3-C_2C_4}\\&+\frac{C_1\left[\zeta\left(x_1,t\right)e^{-2i\kappa_{c2}\Delta x}-\zeta\left(x_3,t\right)/ks_2\right]}{C_1C_3-C_2C_4}\end{aligned} \tag{10}$$

$$\begin{aligned}a_R e^{i(\Delta\omega t+\kappa_1 x_1+\phi_R)}=&\frac{C_3\left[\zeta\left(x_1,t\right)e^{-i\kappa_{c1}\Delta x}-\zeta\left(x_2,t\right)/ks_1\right]}{-2i\left(C_2C_4-C_1C_3\right)}\\&-\frac{C_4\left[\zeta\left(x_1,t\right)e^{-2i\kappa_{c2}\Delta x}-\zeta\left(x_3,t\right)/ks_2\right]}{-2i\left(C_2C_4-C_1C_3\right)}\end{aligned} \tag{11}$$

$$a_I e^{i(\Delta\omega t-\kappa_1 x_1+\phi_I)}=\zeta\left(x_1,t\right)-a_B e^{i(\Delta\omega t-\Delta k_1 x_1+\phi)}-a_R e^{i(\Delta\omega t+\kappa_1 x_1+\phi_R)}. \tag{12}$$

$$\begin{aligned}C_1&=\sin\left(\Delta x\kappa_{c1}\right)\\C_2&=\sin\left[\left(1+\delta\right)\Delta x\kappa_{c2}\right]\\C_3&=e^{-i\left[(1+\delta)\Delta x\kappa_{c2}\right]}-e^{-i\left[(1+\delta)\Delta x\kappa_{c2}\right]}\\C_3&=e^{-i\Delta x\kappa_{c1}}-e^{-i\Delta x\Delta k_{c1}}\end{aligned} \tag{13}$$

The real parts of Eqs. (10), (11), (12) are the time series of the separated waves.

TEST OF THE METHOD BY NUMERICAL RESULTS

To examine the efficiency and validity of the present separation method, numerical example with known incident bound, incident and reflected free waves, is numerically generated. In this test, a water depth h_1 =0.5m is chosen; the beach slope β = 1/40; the spatial distance Δx = 1.0 m. The wave parameters of this test are chosen as follows: wave period, T = 5s, a_I = 0.02m, a_B = 0.02m and a_R = 0.01m. Figure 2 shows calculated results using the present method. The results show that the errors are very small and can be neglected. Figure 3 shows the separation results of another numerical case, using the same wave parameters but at a steeper slope, β = 1/10. It is found that the errors for the case at the beach with slope β = 1/10 is more obvious than that at the beach with slope β = 1/40, indicating that the accuracy of the present method is closely related to the slope of beaches.

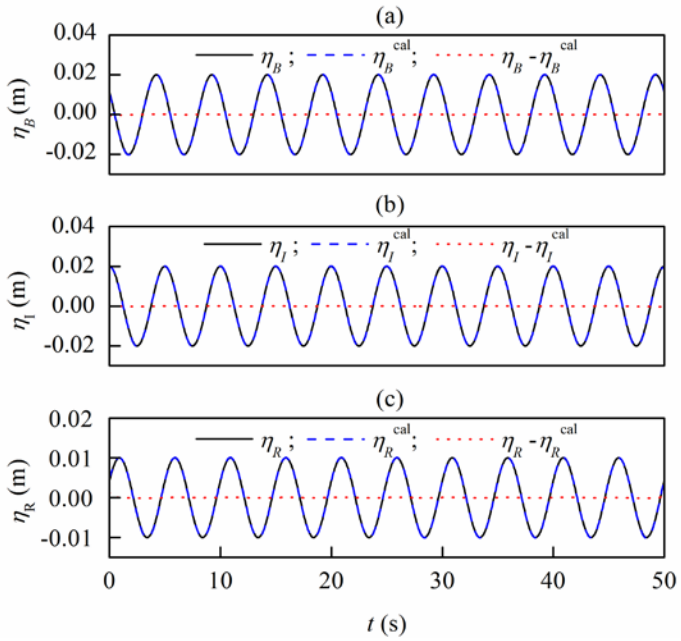

Figure 2. Comparisons between the target and calculated surface elevations of incident bound long waves (a), incident (b) and reflected (c) free long waves at x_1 over a sloping beach with β = 1/40.

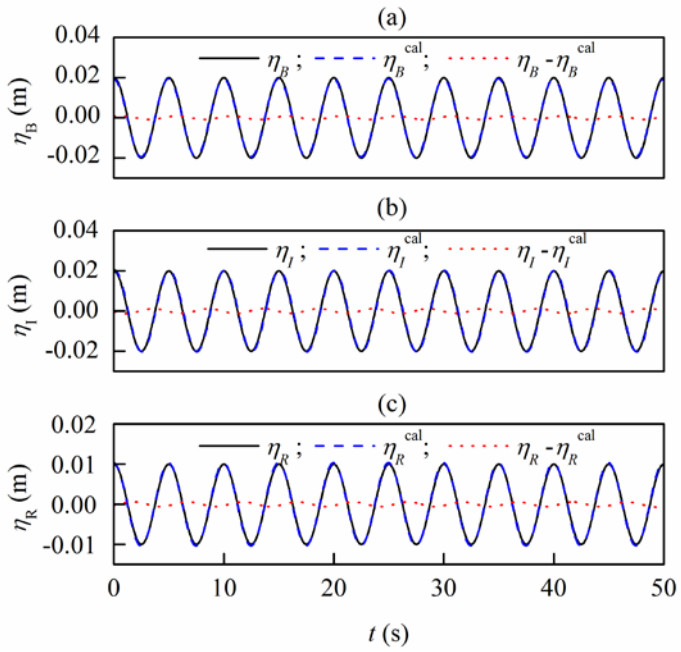

Figure 3. Comparisons between the target and calculated surface elevations of incident bound long waves (a), incident (b) and reflected (c) free long waves at x_1 over a sloping beach with β = 1/10.

To a better understanding of the applicability of the present method, a number of numerical tests are generated at different slope beaches and at different water depths. The wave parameters are the same as the examples shown in Figure 2 and Figure 3. The separation errors for the tests over constant depths are shown in Figure 4. The errors are calculated as $[(a_{tar} - a_{cal})/a_{tar}]*100$, in which a_{tar} is the target amplitude and a_{cal} is the calculated amplitude. The tests show that the errors of the present method are very small over constant depth, even in very shallow water depths.

Figure 5 shows the separation errors over a mild slope beach with β = 1/40. The errors are very small at places where water depth *kh* is larger than 0.2. But, at places where *kh* is smaller than 0.2, the errors exceed 10%, thus this method is invalid. The separation errors for steeper slope beaches over variable water depths are shown in Figure 6 and Figure 7. The results illustrate that the separation errors at steeper beaches are larger than that of milder slope beaches. At shallow water depth, closer gauge locations can improve the separation results. However, at very shallow water depth where *kh* is smaller than 0.2, the present method is invalid, even with a closer spacing gauge location.

The above numerical tests have shown that the present method can give correct results at places where *kh* is larger than 0.2 over both mild and steep slope beaches. In the next section, this new method will be used to study an experiment for the generation of low-frequency waves over a mild slope beach.

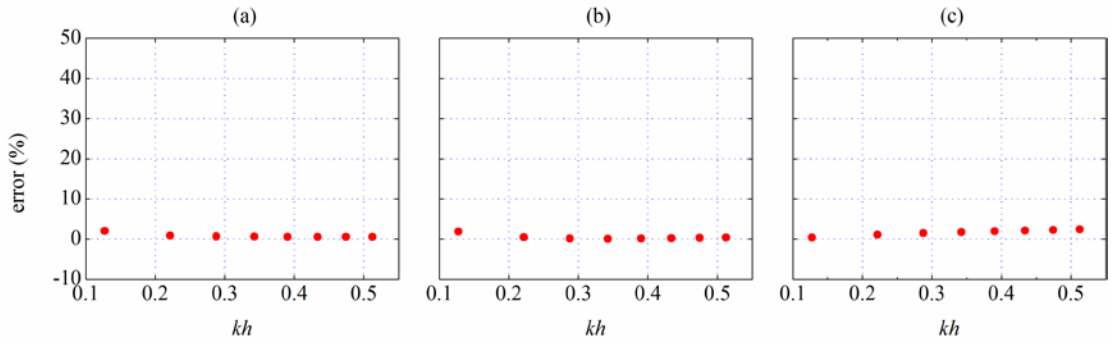

Figure 4. The errors of the calculated results over constant depths; (a) incident bound waves, (b) incident free waves, (c) reflected free waves; Δx_1 = 1m, Δx_2 = 2m.

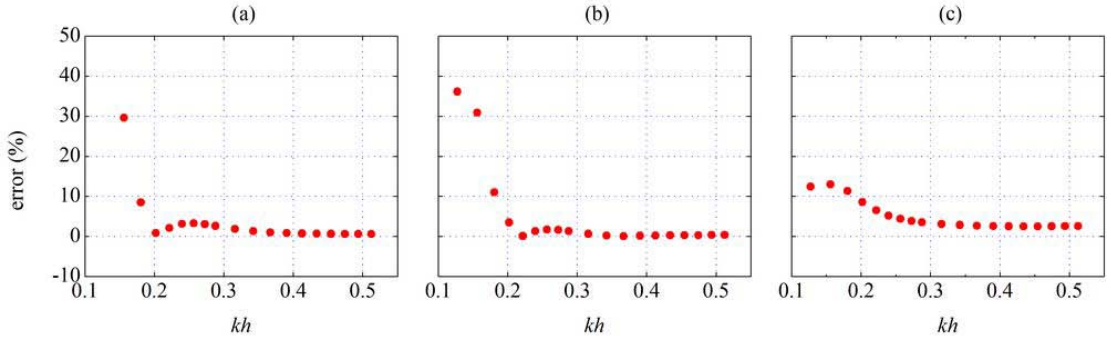

Figure 5. The errors of the calculated results over a slope beach, β = 1/40; (a) incident bound waves, (b) incident free waves, (c) reflected free waves; Δx_1 = 1m, Δx_2 = 2m.

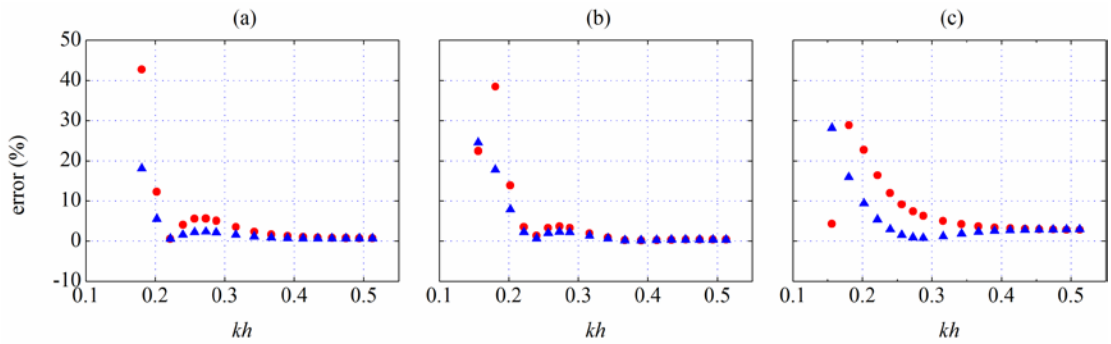

Figure 6. The errors of the calculated results over a slope beach, β = 1/20; (a) incident bound waves, (b) incident free waves, (c) reflected free waves; (●) Δx_1 = 1m, Δx_2 = 2m (▲) Δx_1 = 0.5m, Δx_2 = 1m.

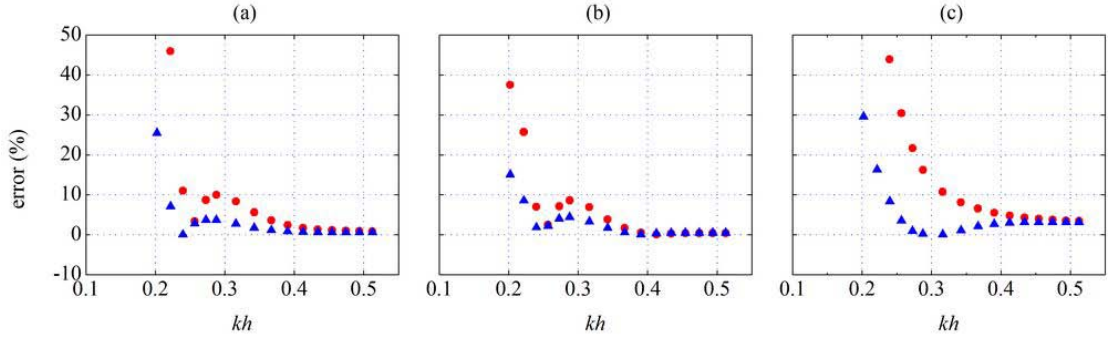

Figure 7. The errors of the calculated results over a slope beach, β = 1/10; (a) incident bound waves, (b)

incident free waves, (c) reflected free waves; (●) Δx_1 = 1m, Δx_2 = 2m (▲) Δx_1 = 0.5m, Δx_2 = 1m.

EXAMPLE OF APPLICATION

The experiments are conducted in the wave flume at the State Key Laboratory of Coastal and Offshore Engineering, Dalian University of Technology, P. R. China. This flume is 50.0m long, 3.0m wide and is used with a working depth of 0.5m. The flume is equipped with a hydraulically driven, piston-type wave generator at one end and a wave absorber at the other. The origin of the *x* axis is fixed at the average position of the wave board and *x* is positive in the incident wave direction. The positive *z*-coordinate points upward from the still water level (SWL). The slope is used in the present experiments are shown schematically in Figure 8. The bottom profile used in the experiments is constructed with a finished smooth concrete surface overlying a sand filled template. The beach profile is a mild slope (1:40) with a one-meter long approach slope (1:10) that spans from *x* = 8m through *x* = 21m.

The surface elevations on the bathymetry are recorded with 22 capacitance wave gauges; their positions are delineated in Figure 8. The gauges are positioned with a 1.0m or 2.0mspacing across the offshore horizontal profile and across the offshore part of the slope. To increase spatial resolution of the measurements in the vicinity of wave breaking, gauge density is increased to 0.5m near the discontinuity in slope. The control signal to the wave paddle is computed using a second-order wave-maker theory (Schäffer, 1996), which significantly suppresses the spurious free waves.

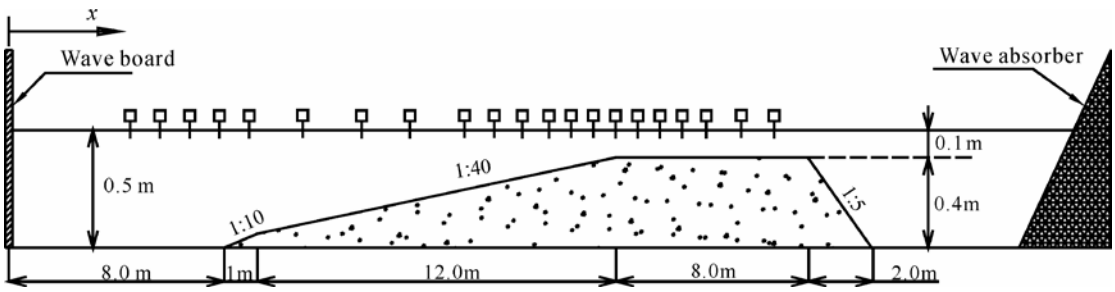

Figure 8. Schematic drawing of the experimental setup

In the present study, four bichromatic wave groups with same amplitude modulation rate a_1/a_2, but different group frequencies $f_g = f_2 - f_1$ are considered here; each record is 102.4 s in length with sample interval 0.025 s. The parameters of the wave groups are shown in Table 1. Before the separation procedure, the measured low-frequency waves are obtained by a band-pass filter.

Figure 9 and Figure 10 show the separated bound low-frequency waves at the offshore locations (*x* = 7m). For comparison, the theoretical results of Longuet-Higgins and Stewart (1962) and the measured short waves are also shown in these figures. The amplitudes and phases of the calculated bound long waves are consistent well with the theoretical results, which is further proving that the present method is valid.

Table 1. Parameters of the bichromatic wave groups

Case	f_1 (Hz)	f_2 (Hz)	a_1 (m)	a_2 (m)	f_g (Hz)	a_1/a_2
1	0.90	1.100	0.0185	0.0205	0.20	0.9
2	0.0875	1.125	0.0185	0.0205	0.25	0.9

3	0.085	1.150	0.0185	0.0205	0.30	0.9
4	0.825	1.175	0.0185	0.0205	0.35	0.9

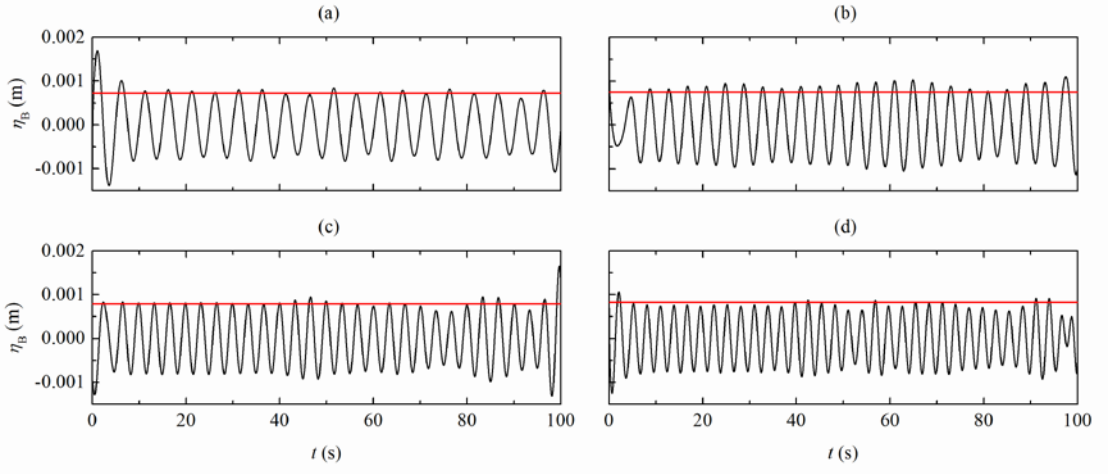

Figure 9. The time series of the bound long waves at *x* = 7m for the experimental cases; the red horizontal lines are the theory results of Longuet-Higgins and Stewart (1962); (a) Case 1, (b) Case 2, (c) Case 3, (d) Case 4.

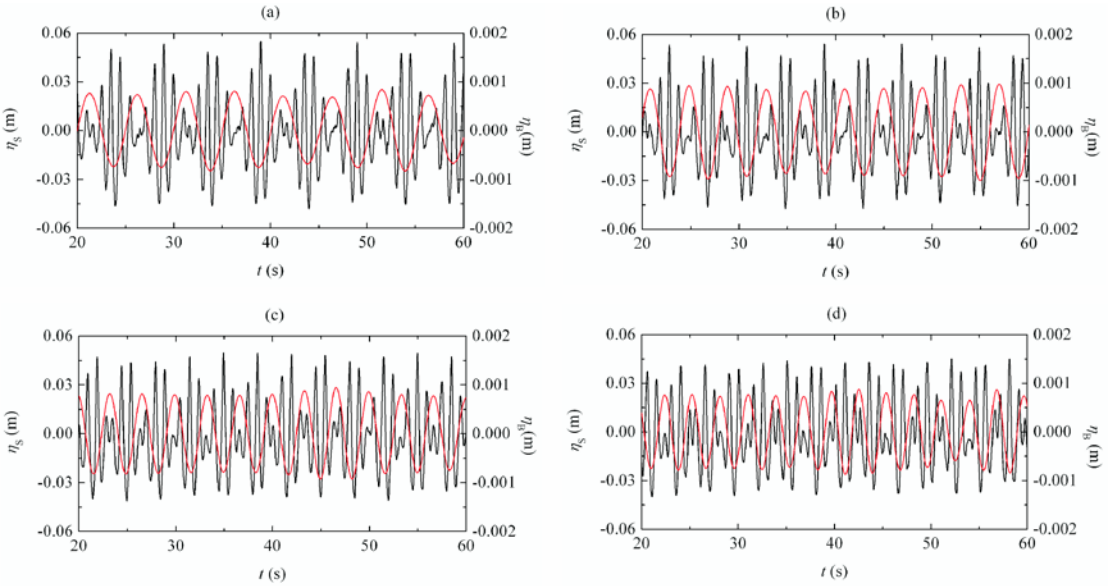

Figure 10. The measured short wave groups and the corresponding bound waves at *x* =7m; (a) Case 1, (b) Case 2, (c) Case 3, (d) Case 4.

Figure 11 and Figure 12 show the calculated results at several locations along the beach for Case 1 and 3, respectively. The amplitudes of the bound wave increase as water depth decrease and the time series are almost uniform before wave breaking. After breaking, the bound wave amplitudes decrease and the time series are not uniform anymore. The incident free waves are almost not change before initial breaking, and increase sharply in the surf zone. Meanwhile, the reflected free waves are almost not change along the shore. The results indicate that the release of bound long waves is the main mechanics of generation of low-frequency waves in the mild slope beach, which is consistent with the results of Dong *et al*. (2009).

The additional lag $\Delta\phi = \phi - \pi$ can be obtained by a correlation calculation, where ϕ is the phase lag of the bound long wave behind the short wave envelop. In this study, the additional lags $\Delta\phi = 2\pi f_g$, where τ is the lag time of the maximum negative correlation between the bound long waves and the short-wave group envelops. The cross-shore variations of the additional lags for the experimental cases are shown in Figure 13. This shows that before initial breaking, the phase lags between bound long waves and envelops is close to zero. After initial breaking, the phase lags change sharply, where the bound long waves are behind the short waves about $\pi/2$, while in the inner surf zone, the phase lags are about π, which is similar to the conclusion of Battjes *et al*. (2004).

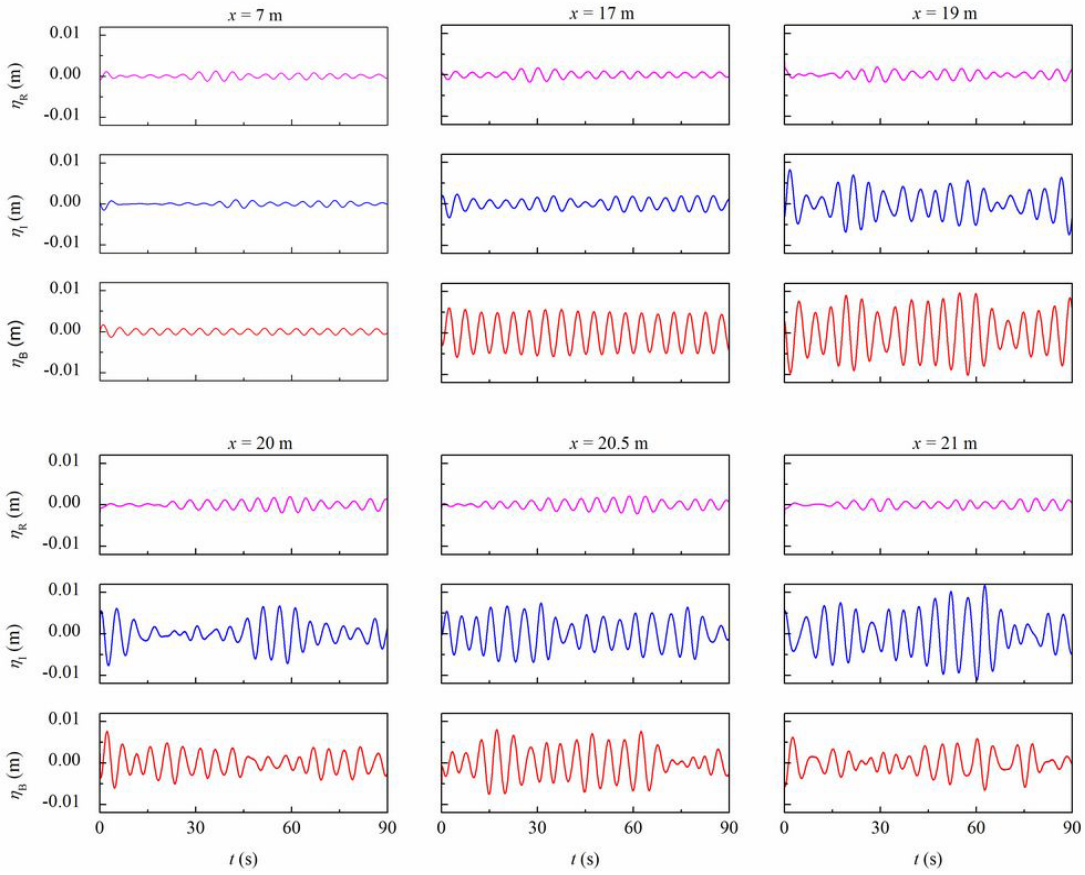

Figure 11. The separation results at several locations along the flume for Case 1； initial breaking occurs at *x* = 19m.

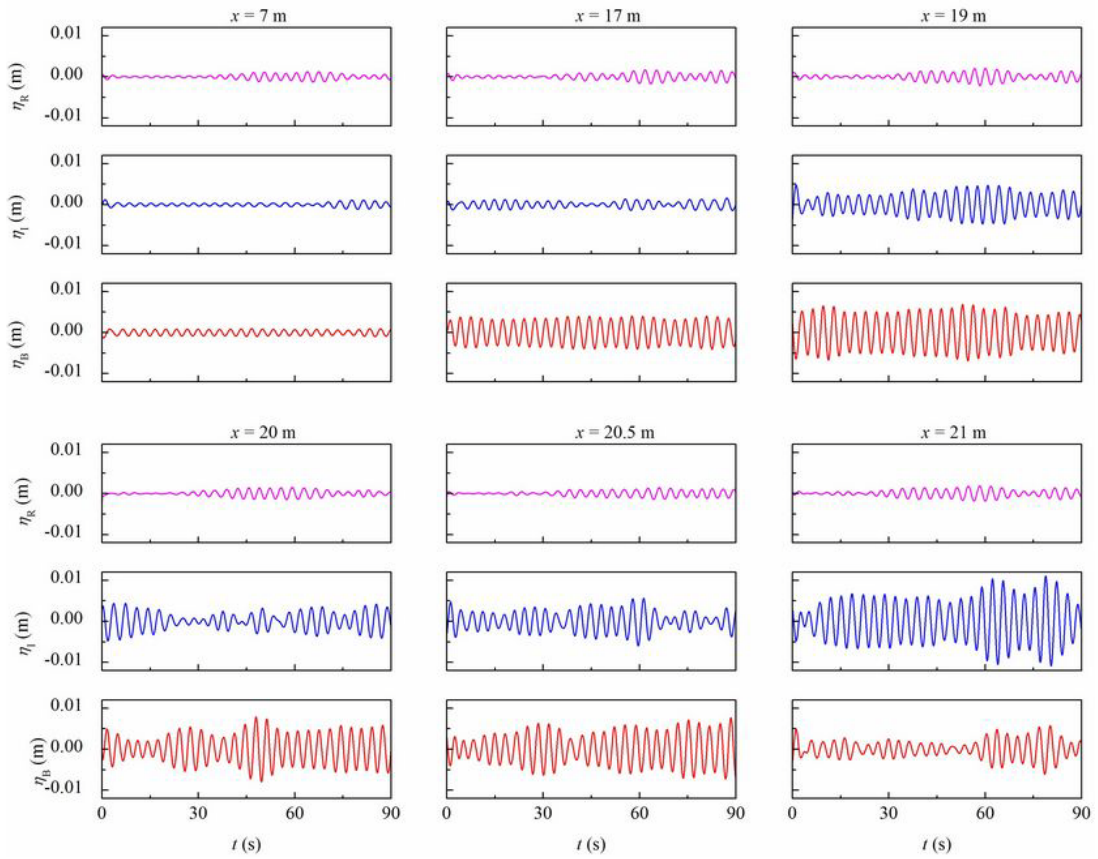

Figure 12. The separation results at several locations along the flume for Case 3; initial breaking occurs at *x* = 19m.

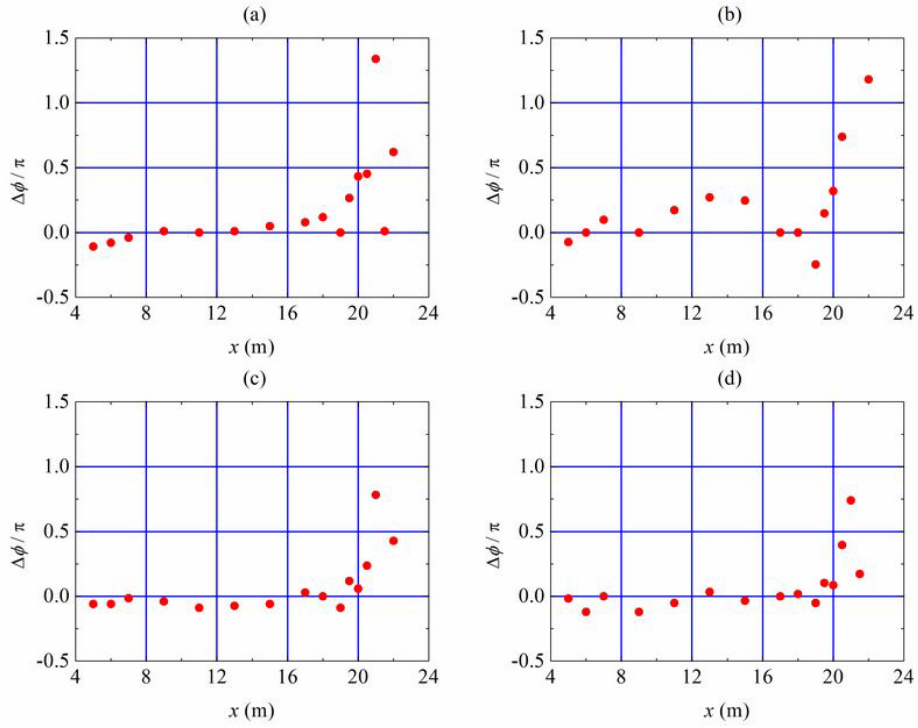

Figure 13. The additional phase lags of the bound long waves behind the short wave groups along the wave flume.

CONCLUSIONS

A new 2D method for separating low-frequency waves in real time domain over sloping bathymetries is proposed by constructing the analytical signals of the measured waves. The efficiency and accuracy of this method are demonstrated using numerically simulated data. The results show that the present method can give accurate results at relative water depth (kh) larger than 0.2. At shallow water depth ($kh < 0.2$), the errors is larger than 10%, so this method is invalid.

Using the present method, experiments of low-frequency waves generated by bichromatic wave groups over at mild slope beach are studied. The separated results show that the release of bound subharmonic waves is the dominant mechanics of generation of surf beat at mild slope beaches. The study of the local correlations between the incident bound low-frequency waves and the short wave envelopes along the tank shows that the phase lags between bound long waves and envelops is close to 0 before initial breaking, while the phase lags change sharply after initial breaking. The bound long waves are behind the short waves about $\pi/2$ at the initial breaking point, while the phase lags are about π in inner surf zone,, which is consistent with the previous experimental studies.

ACKNOWLEDGMENTS

This research is supported financially by the National Nature Science Foundation (Grant Nos. 50921001, 51009024), the Specialized Research Fund for the Doctoral Program (No. 20100041110005), the China Postdoctoral Science Foundation funded project (No. 20100481231) and the Fundamental Research Funds for the Central Universities.

REFERENCES

Bakkenes, H.J. 2002. Observation and separation of bound and free low-frequency waves in the nearshore zone, in Faculty of Civil Engineering and Geosciences. Delft University of Technology: Delft.

Baldock, T.E., D.A., Huntley, P.A.D., Bird, T.O., Hare, and G.N., Bullock. 2000. Breakpoint generated surf beat induced by bichromatic wave groups. *Coastal Engineering*. 30 (2-4): 213-242.

Battjes, J.A., Bakkenes, H.J., Janssen, T.T., van Dongeren, A.R. 2004. Shoaling of subharmonic gravity waves. *J. Geophys. Res.*, 109(C2): C02009.

Bowers, E.C.. 1977. Harbour resonance due to set-down beneath wave groups. *Journal of Fluid Mechanics*. 79: 71-92.

Cohen, L. 1995. *Time Frequency Analysis: Theory and Applications*. Prentice Hall Englewood Cliffs, New Jersey.

Dong, G.H., X.Z., Ma, M., Perlin, Y.X., Ma, B., Yu, and G., Wang. 2009. Experimental Study of long wave generation on sloping bottoms. *Coastal Engineering*, 56(1), 82-89.

Kamphuis, J.W. 2000. Designing for low frequency waves. *Proceedings of 27th International Conference on Coastal Engineering*. Sydney, Australian. 1434-1447.

Kostense, J.K. 1984. Measurements of surf beat and set-down beneath wave groups. *Proceedings of 19th International Conference on Coastal Engineering*. Houston, USA. 724-740.

Longuet-Higgins, M.S. and R.W., Stewart. 1962. Radiation stress and mass transport in gravity waves with application to ‘surfbeat’. *Journal of Fluid Mechanics*. 13: 481-504

Mallat, S. 1999. *A Wavelet Tour of Signal Processing*. Academic Press.

Nagai, T., N., Hashimoto, T., Asai, et al. 1994. Relationship of a moored vessel in a harbor and a long wave caused by wave groups. *Proceedings of 17th International Conference on Coastal Engineering*. Kobe, Japan. 847-861.

Schäffer, H.A. 1993. Second-orderwavemaker theory for irregularwaves.Ocean Engineering. 23 (1), 47–88.

Symonds, G.D.A., D.A., Huntley, and A.J., Bowen. 1982. Two-dimensional surf beat-long-wave generation by a time-varying breakpoint. *Journal of Geophysical Research*. 87(C1): 492-498.

Yu, J. and C.C., Mei. 2000. Formation of sand bars under surface waves. *Journal of Fluid Mechanics*. 416: 315-348.